The effects of surface curvature on the adsorption of surfactants at the solid-liquid interface

Post-print of peer-reviewed article published by the Royal Society of Chemistry.
Published article available at: http://dx.doi.org/10.1039/C3CP50585E

Cite as:
Farrow, M. R., Camp, P. J., Dowding, P. J., & Lewtas, K. (2013). The effects of surface curvature on the adsorption of surfactants at the solid-liquid interface.*Physical chemistry chemical physics*, 15(28), 11653-11660.

Manuscript received: 07/02/2013; Accepted: 14/04/2013; Article published: 05/05/2013

The effects of surface curvature on the adsorption of surfactants at the solid–liquid interface**†

M.R. Farrow,[1] P.J. Camp,[2,*] P.J. Dowding[3] and K. Lewtas[3]

[1]Department of Chemistry, Kathleen Lonsdale Materials Chemistry, University College London, 20 Gordon Street, London WC1H 0AJ, UK.

[2]EaStCHEM, School of Chemistry, Joseph Black Building, University of Edinburgh, West Mains Road, Edinburgh, EH9 3JJ, UK.

[3]Infineum UK Ltd, PO Box 1, Milton Hill, Abingdon OX13 6BB, UK.

[*]Corresponding author; e-mail: philip.camp@ed.ac.uk

[**]This research was supported by Infineum UK Ltd through a postdoctoral fellowship to M. R. F. and funds for the purchase of computer hardware.

[†]Celebrating 300 years of Chemistry at Edinburgh.

Graphical abstract:

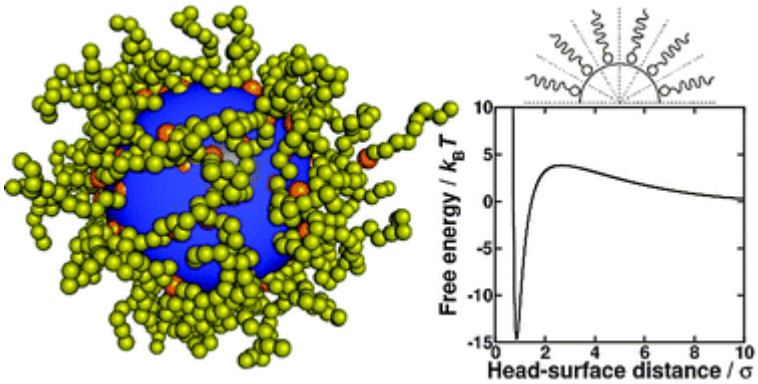

Summary:
The adsorption of surfactant on a colloidal surface is measured as a function of coverage and curvature.

Abstract

The adsorption of surfactants from dilute oil solutions on to solid surfaces is studied as a function of surface curvature and surface coverage. Coarse-grained molecular models, computer simulations, and umbrella sampling are used to compute the dependence of the free energy of adsorption on to a spherical colloid surface with radius R. It is shown that for fixed surface coverage, and with all other things being equal, the free energy of adsorption decreases with decreasing R. For fixed surface curvature, the free energy of adsorption increases with increasing surface coverage. These trends arise from the excluded-volume interactions between the surfactant tails. The dependence on surface curvature is due to the geometrical effect of there being more free volume for the surfactant tails with a smaller colloid radius. The consequences of these effects on equilibrium partitioning are examined. It is shown that for surfactants adsorbed on small-colloid and large-colloid surfaces in mutual equilibrium with a dilute solution, the surface coverage of the small particles is significantly greater. The implications for industrial applications are discussed and could be significant.

1. Introduction

The adsorption of surfactants onto the interface between a solid and a liquid solution is important in many applications, including lubrication, detergency, wetting, and emulsions. The most common examples involve aqueous solutions of surfactants with hydrophobic tail groups and polar or ionic head groups in contact with a planar solid surface or the surfaces of solid colloidal particles. In this situation, the surfactants may self-assemble to form micelles and other structures, and the interplay between self-assembly and surface adsorption can give rise to interesting structural and kinetic effects. Probably the best-studied situation is the adsorption of ionic and non-ionic surfactants (and their mixtures) on to hydrophilic silica surfaces.[1–14] In many of these studies, the silica is colloidal, with radii on the order of 100 Å. The surfactants may either form uniform bilayers, defective bilayers, or surface micelles, and the presence of these adsorbed layers has been found to play a significant role in the effective interactions between the colloidal particles. Central to these phenomena is the interplay between the radius of curvature of the solid surface and the spontaneous curvature of the micelles, which is controlled by the molecular architecture of the surfactant.[3,7,9–11,13]

Despite its industrial relevance to the lubricant industry, the adsorption of amphiphilic molecules on to inorganic surfaces from oil-based solutions has received less detailed attention. One important example is an overbased detergent, this being a combination of inorganic particles (such as calcium carbonate) solubilised with ionic surfactants. The inorganic particles are relatively small, with radii in the region of 10–50 Å. These systems are added to engine oils to neutralise corrosive acidic products of sulphur and oil oxidations. Bearchell *et al.* studied the detailed structures of various surfactants

adsorbed on calcium carbonate particles, using Langmuir trough, Langmuir–Blodgett, and ellipsometry experiments, in combination with molecular-dynamics simulations.[15,16] In typical applications, the surfactant tail groups are aliphatic and hence solvophilic. The head groups are polar or ionic and hence solvophobic, which favours adsorption on to typical inorganic surfaces. Potentially, surfactants could self-assemble to form reverse micelles in solution, and one would then have to consider the particle curvature and the micellar spontaneous curvature, just as in aqueous solutions. As an example, small-angle X-ray scattering studies show that ~10 wt% glycerol monooleate in alkanes forms ellipsoidal reverse micelles, and that the presence of a small amount of water (~1 wt%) promotes micelle formation.[17] In general, though, for typical surfactants (with 'small' head groups and 'large' hydrophobic tails) reverse micelle formation in non-aqueous solvents is far less common than micelle formation in water. Hence, the surfactant may form a single layer on the inorganic surface without prior or subsequent self-assembly.[15,16]

Molecular simulations provide valuable insights on the microscopic structures and thermodynamics of adsorbed layers. For instance, atomistic molecular dynamics simulations may be used to study the thermodynamics of adsorption of molecules on to planar inorganic surfaces,[18] organic solids,[19] membranes,[20] or various carbon surfaces.[21] Bearchell *et al.* used atomistic simulations to examine the molecular structure of overbased detergents.[15,16] Alternatively, coarse-grained molecular models and Monte Carlo simulations may be used to study the more demanding problem of self-assembly and adsorption.[22,23] This work is focused on the role of the surface curvature on the thermodynamics of surfactant adsorption at the solid–liquid interface. This should be important for situations where there is competition between adsorption at surfaces of different curvature. An obvious example is an oil-based solution of surfactants in equilibrium with the adsorbed layers on the rough surfaces of a container and the curved surfaces of colloidal particles dispersed in the solution. Another example would be the partitioning between different dispersed particles in a highly polydisperse system.

In this work, the effects of surface curvature are isolated by constructing coarse-grained models of typical surfactant molecules, and solid spherical surfaces. The interactions between the surfactants and the surfaces are parametrised in such a way that the only variables are the surface coverage and the radius of curvature of the surface; this is equivalent to making all surfaces from the same material. The surfactant solution is considered to be so dilute that (i) the solution is essentially ideal, and (ii) there is no self-assembly of the surfactants to form reverse micelles (as is often the case in non-aqueous solvents). The thermodynamic functions characterising adsorption are calculated using Langevin dynamics simulations and umbrella sampling. Specifically, the reversible work (free energy change) of bringing the head group from infinitely far away to the surface is computed as a function of the perpendicular distance.[24] This is also known as the potential of mean force (PMF).[25] The PMF is essentially a free energy at a constrained head–surface distance since all other degrees of

freedom associated with the surfactant tail and the adsorbed surfactants are 'integrated out'.[26] It is shown that the adsorption of a surfactant molecule on to a surface of fixed coverage becomes less favourable with increasing radius. This means that the higher the surface radius, the higher the solution concentration must be to achieve the same surface coverage. For a surface of fixed radius, adsorption becomes less favourable with increasing surface coverage. These variations with coverage and radius reflect the interplay between the intermolecular interactions between the surfactants and their compatibility with the surface structure [see Figure 2(b) and (c)]. The dependences of the thermodynamic functions on the material parameters allow an assessment to be made of the likely equilibrium partitioning of surfactants between surfaces of different curvature at mutual equilibrium with a solution.

The situation considered in this work (adsorption on to particles dispersed in oil) is significant different from the aqueous systems referred to above. Firstly, the typical particle sizes in overbased detergent systems are small, so the curvature of the particle surface is likely to be important. Secondly, (reverse) micelle formation of surfactants in oil is generally much less common than in aqueous media, and so a competition between spontaneous micelle curvature and particle curvature is not likely to be an important consideration. This provides a straightforward situation which can be considered in detail. Finally, oil-based systems have received far less attention to date, despite their industrial importance: in particular, there has not yet been an in-depth, systematic survey of adsorption on to colloidal particles of different sizes. For all of these reasons, the current work provides a new contribution to the detailed study of surfactant adsorption from oil and on to spherical colloidal surfaces.

This paper is organised as follows. In Section 2, the coarse-grained model is defined. In Section 3 the basic simulation approach is described, and the method for calculating adsorption is detailed. The results are presented in Section 4, focused on the change in free energy on adsorbing a surfactant molecule on to the surface, the adsorption isotherms, and the consequences for the partitioning between surfaces of different curvature. The overall conclusions are presented in Section 5.

2. Model and methods

A surfactant was modelled as a chain of twelve solvophilic coarse-grained beads (the tail groups), and one solvophobic and 'surface-philic' head bead (the head group). The solvent is implicit. The solvophobic groups experience a mutual attraction and an attraction to the surface. The solvophilic groups are ambivalent, and all of their interactions are made purely repulsive (excluded-volume interactions). All non-bonded interactions between beads were expressed in terms of the Lennard-Jones (LJ) pair potential

$$u_{LJ}(r) = 4\varepsilon\left[\left(\frac{\sigma}{r}\right)^{12} - \left(\frac{\sigma}{r}\right)^{6}\right] \quad (1)$$

where r is the distance between two beads, and ε and σ are the energy and bead diameter, respectively. Attractive head–head interactions were represented by the LJ potential cut and shifted at $r_c = 2.5\sigma$. Repulsive tail–tail and head–tail interactions were given by the LJ potential cut and shifted at the minimum $r_{min} = 2^{1/6}\sigma$, *i.e.*, the Weeks–Chandler–Andersen (WCA) potential, u_{WCA}.[27] The interaction between bonded beads was a combination of the WCA potential and a finitely extensible non-linear elastic potential

$$u_b(r) = -\frac{1}{2}\kappa_b r_b^2 \ln\left[1 - \left(\frac{r}{r_b}\right)^2\right] \quad (2)$$

where $\kappa_b = 30\varepsilon/\sigma^2$ and $r_b = 1.5\sigma$ are conventional choices.[28–30] The interactions between non-bonded and bonded beads are shown in Figure 1(a) and (b), respectively. Figure 1(b) shows that the combination of u_b and u_{WCA} gives a bonding potential with an equilibrium distance of about 1σ.

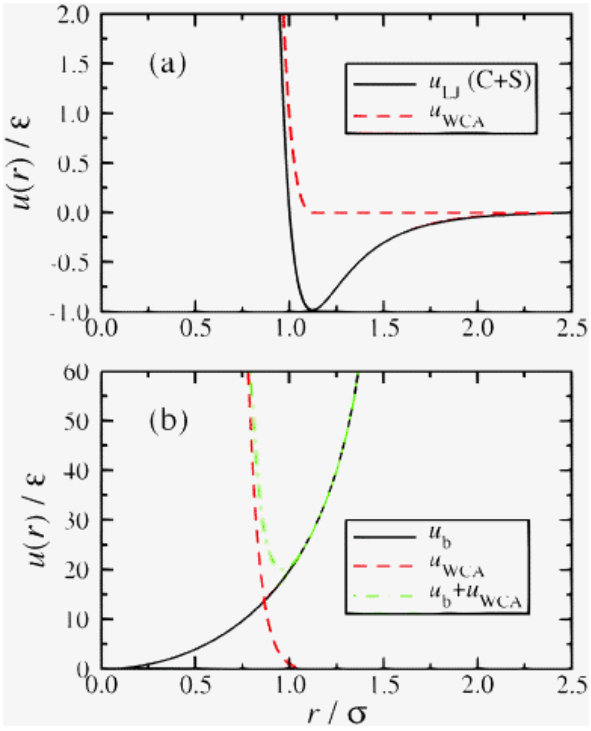

Figure 1. (a) Interaction potentials for non-bonded beads: (black solid line) head–head interactions (u_{LJ} cut-and-shifted at $r_c = 2.5\sigma$); (red dashed line) head–tail and tail–tail interactions (u_{WCA}). (b) Interaction potentials for bonded beads: (black solid line) finitely extensible non-linear elastic potential (u_b); (red dashed line) head–tail and tail–tail interactions (u_{WCA}); (green dot-dashed line) total interaction ($u_b + u_{WCA}$).

Colloidal surfaces were modelled as structureless spheres. The interactions between surfactant beads and the surfaces were given in terms of the potential

$$\varphi_s(z) = \frac{2\pi\varepsilon_s}{3}\left[\frac{2}{15}\left(\frac{\sigma}{z}\right)^9 - \left(\frac{\sigma}{z}\right)^3\right] \qquad (3)$$

where z is the perpendicular distance of the bead from the surface, and ε_s is an energy parameter. $\varphi_s(z)$ is obtained by integrating the LJ potential between a bead and a *planar* surface,[31,32] but it is adopted here also for colloid surfaces to give a consistent bead-surface potential amongst all of the systems studied. The head groups are assumed to be attracted to the surface, and hence the potential is $\varphi_s(z)$. For the tail groups, the bead-surface potential was $\varphi_s(z)$ cut and shifted at its minimum $z_{min} = (2/5)^{1/6}\sigma$ to give a purely repulsive interaction. Of course, this is a crude model that ignores important effects such as specific interactions, and the effects of solvent restructuring on solute adsorption, but it should allow a systematic study of the effects of surface curvature.

For a typical straight-chain surfactant molecule with a C_{24} backbone and a head group rendered as a chain of thirteen coarse-grained beads, each bead roughly corresponds to a group of two CH_2 units. If one bead equates to a group with formula CH_3CH_3, then the LJ ε and σ can be estimated from the known critical properties of ethane. From ref. 33, the critical temperature is T_c = 305 K and the critical molar volume is V_c = 146 cm^3 mol^{-1}. For the cut-and-shifted LJ fluid, $k_BT_c/\varepsilon = 1.08$ and $V/N\sigma^3 = 3.11$.[34] These data imply that $\sigma \simeq 4$ Å and $\varepsilon/k_B \simeq 282$ K. Spherical colloids with radii of R/σ = 2, 4, 6, 8, and 10 were considered. In real units, these diameters lie in the range $16 \leq 2R \leq 80$ Å, which is absolutely typical for overbased detergent systems.

N surfactant molecules were packed on to the surfaces to give nominal coverages in the range $0 \leq \Gamma\sigma^2 \leq 0.50$, where $\Gamma = N/(4\pi R^2)$. Systems were simulated without boundaries since the surfactants were sufficiently strongly adsorbed to avoid desorption on the simulation timescale. The thermodynamics of adsorption was studied under the assumption of an ideal surfactant solution, and so it was not necessary to simulate this explicitly. A typical simulation snapshot is shown in Figure 2(a).

(turn to next page →)

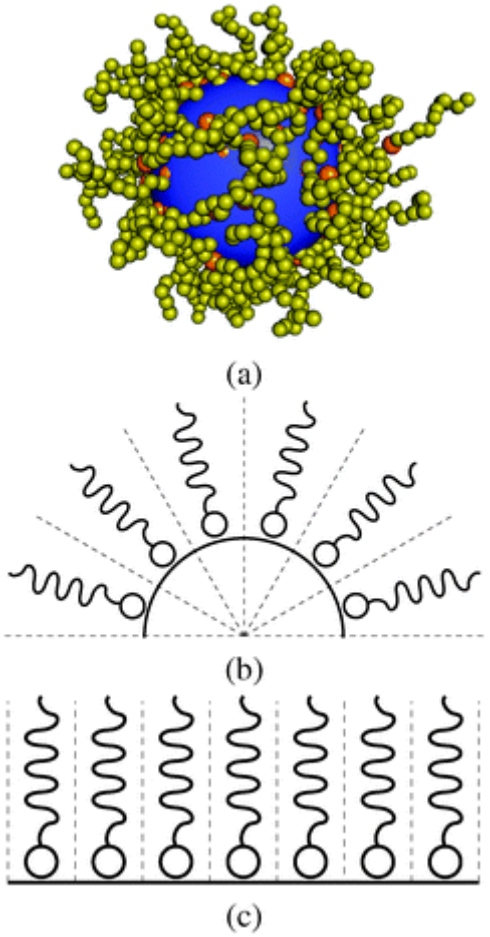

Figure 2. (a) Simulation snapshot of a colloid of radius $R = 8\sigma$ with surface coverage $\Gamma\sigma^2 = 0.101$. The surfactant molecules are represented with yellow beads for tail groups and orange beads for head groups. A selected surfactant molecule is anchored away from the surface to carry out umbrella-sampling. (b) and (c) Schematic diagrams of surfactant molecules adsorbed on (b) a curved surface and (c) a planar surface with equal surface coverages. The dashed lines indicate the volume per surfactant tail.

3. Computer simulations

The model systems were simulated using Langevin dynamics in which the surfactants in the fluid experience random and drag forces (mimicking the Brownian forces in a solvent) and the conservative interaction forces derived from the potentials given above. The equation of motion for bead i reads

$$m\ddot{\boldsymbol{r}}_i = -\nabla U_i - \gamma m\dot{\boldsymbol{r}}_i + \boldsymbol{W}_i(t) \qquad (4)$$

where m is the bead mass (assumed to be the same for all beads), $\boldsymbol{r}_i$ is the position vector of bead i, γ is the Langevin friction coefficient, $\boldsymbol{W}_i(t)$ describes the random, Brownian forces of the solvent acting on

the bead, and U_i is the potential energy of the bead from which the force is derived. The total potential energy is given by a sum over pairwise additive interactions. $\boldsymbol{W}_i(t)$ is represented by Gaussian white noise that satisfies the fluctuation-dissipation theorem:[35]

$$\langle \boldsymbol{W}_i(t) \cdot \boldsymbol{W}_j(t') \rangle = 6k_B T m \gamma \delta_{ij} \delta(t - t') \qquad (5)$$

The simulations were conducted in reduced units. The reduced temperature is given by $T^* = k_B T/\varepsilon$ and all simulations were conducted at $T^* = 1$ since ε is in the region of 282 K. At room temperature $k_B T = \varepsilon \simeq 2.5$ kJ mol^{-1}; the interactions that bind surfactant head groups to surfaces are typically a few tens of kilojoules per mole, and so the bead–surface interaction parameter ε_s was set equal to 10ε. The basic unit of time is $\tau = (m\sigma^2/\varepsilon)^{1/2}$; with $\sigma = 4$ Å, $m = 30$ amu, and $\varepsilon = k_B T$, this corresponds to $\tau = 1.2$ ps at room temperature. The time-step for the dynamics simulations was $\delta t = 0.001\tau$ and the friction coefficient was $\gamma = 0.5\tau^{-1}$.

Simulations were used to estimate the free energy change of bringing a single surfactant molecule to a height z above a surface with coverage Γ, and thereby to calculate the adsorption isotherm. The theory is outlined first, and the simulation details are given afterwards.

3.1. Adsorption

Consider the process of adsorbing a molecule on to a surface with coverage Γ. It is assumed that the surfactant molecules adsorbed on the surface are in equilibrium with surfactant in bulk solution, and that the concentration of the bulk solution (c_0) is sufficiently low that the solution can be considered ideal. In this case, the chemical potential of the surfactant in bulk solution is given by

$$\mu_0 = \mu^\ominus + k_B T \ln\left(\frac{c_0}{c^\ominus}\right) \qquad (6)$$

where $\mu^\ominus$ is the standard chemical potential at standard concentration $c^\ominus$. Now consider the chemical potential of a surfactant molecule adsorbed at a height z that is taken to be the perpendicular separation between the surface and the head group of the surfactant; this is written in the form

$$\mu(z) = \mu^\ominus + k_B T \ln\left[\frac{c(z)}{c^\ominus}\right] + w(z) \qquad (7)$$

where $c(z)$ is the local concentration of surfactant head groups, and $w(z)$ is the change in excess free energy on transferring a surfactant from an ideal bulk solution remote from the surface ($z \rightarrow \infty$) to the

position z from the surface with coverage Γ. Being an excess property, $w(z)$ arises from the interactions with the other surfactants and the surface. At chemical equilibrium, $\mu(z) = \mu_0$ and so

$$c(z) = c_0 \exp[-\beta w(z)] \qquad (8)$$

where $\beta = 1/k_B T$. The total adsorbed number of molecules per unit area of surface is given by

$$\Gamma = \frac{1}{4\pi R^2} \times 4\pi \int_0^{z^*} (R+z)^2 c(z) \mathrm{d}z$$
$$= c_0 \int_0^{z^*} \left(1+\frac{z}{R}\right)^2 \exp[-\beta w(z)] \mathrm{d}z \equiv c_0 K(\Gamma) \qquad (9)$$

where z^* is a dividing height between adsorbed and desorbed states (to be discussed below). A similar expression could also be used to determine the excess adsorption, Γ_{ex}:

$$\Gamma_{ex} = \frac{1}{4\pi R^2} \times 4\pi \int_0^{z^*} (R+z)^2 [c(z) - c_0] \mathrm{d}z$$
$$= c_0 \int_0^{z^*} \left(1+\frac{z}{R}\right)^2 \left[\mathrm{e}^{-\beta w(z)} - 1\right] \mathrm{d}z. \qquad (10)$$

The total adsorption Γ is fixed in the current simulations and so eqn (9) is most useful. Results similar to eqn (9) have been derived before for the adsorption at radius R for a spherical liquid droplet in equilibrium with its vapour,[36] and for the adsorption of a molecule on to a membrane.[20] The adsorption isotherm is defined by

$$c_0 = \frac{\Gamma}{K(\Gamma)}. \qquad (11)$$

The smaller the value of $K(\Gamma)$, the higher the solution concentration has to be to achieve surface coverage Γ at equilibrium. $K(\Gamma)$ is therefore a kind of equilibrium constant for adsorption.

For very small particles, the equilibrium distance of a head group from the surface ($\sim\sigma$) is significant compared to the particle radius, and hence the actual concentration of adsorbate in the adsorbed layer will be less than the number of particles per unit area of colloid surface. To compare the effects of particle curvature it is important to consider a surface concentration that reflects the true packing density of head groups near the surface. For surfactants at a height z from the particle surface, the surface area over which they are distributed is $1/4\pi(R+z)^2$. An effective surface concentration Γ_{eff} can therefore be defined as

$$\Gamma_{\text{eff}} = 4\pi \int_0^{z^*} (R+z)^2 c(z) \frac{1}{4\pi(R+z)^2} \mathrm{d}z$$
$$= c_0 \int_0^{z^*} \exp[-\beta w(z)] \mathrm{d}z \qquad (12)$$

where eqn (8) has been inserted for $c(z)$. Comparing eqn. (9) and (12) shows that

$$\frac{\Gamma_{\text{eff}}}{\Gamma} = \frac{1}{K(\Gamma)} \int_0^{z^*} \mathrm{e}^{-\beta w(z)} \mathrm{d}z. \qquad (13)$$

This ratio is equal to unity for a planar surface, and decreases with decreasing particle radius R. Ignoring the effects of the tails, this ratio can be approximated using $w(z) = \varphi_s(z)$.

3.2. Umbrella sampling

From the reversible-work theorem,[24] $w(z)$ can be written in the form

$$w(z) = -k_B T \ln\left[\frac{P(z)}{P_0(z)}\right] \qquad (14)$$

where $P(z)$ is the probability of the head group of a selected surfactant being found at height z above the surface, and $P_0(z) \propto 4\pi(R + z)^2$ is the corresponding probability in an ideal solution. [This relation also follows from eqn (8).] It is interesting – and numerically convenient – to measure the function

$$\Delta w(z) = w(z) - \varphi_s(z) = -k_B T \ln\left[\frac{P'(z)}{P_0(z)}\right] \qquad (15)$$

where $P'(z) \propto P(z) \exp[\beta\varphi_s(z)]$ is the probability distribution when there is no head–surface interaction for the selected molecule. $\Delta w(z)$ is the contribution to the free energy arising from head–head, head–tail, and tail–surface interactions, but not the head–surface interaction for the selected molecule. $P'(z)$ was measured using umbrella sampling[37] with a window potential given by

$$\varphi_u(z) = \frac{1}{2}\kappa_u (z - z_u)^2 \qquad (16)$$

so that the measured biased distribution is equal to $P'_u(z) \propto P'(z) \exp[-\beta\varphi_u(z)]$ The portions of $P'(z)$ obtained from different windows of z were concatenated and inserted in to eqn. (14) and (15) so that $w(z)$ and $\Delta w(z)$ are smooth and tend to zero as $z \to \infty$. In this work, the biased simulations were

performed with spring constant $\kappa_u = 10\varepsilon\sigma^{-2}$ and in equally spaced windows centered at $z_u/\sigma = 1, 2, 3, \ldots$.

4. Results

4.1. Free energy of adsorption

Figure 3 shows free-energy profiles for the adsorption of single surfactant molecules on to spherical surfaces with radii $R = 2\sigma$ and 10σ, and with various coverages Γ. Figure 3(a) shows results for $R = 2\sigma$ and $\Gamma\sigma^2 = 0.517$. The points represent $\beta\Delta w$ on a discrete grid as extracted from simulations. $\beta\Delta w$represents all interactions *except* for the head–surface interaction for the selected bead, and because it is dominated by the tail–tail excluded-volume interactions, it is purely repulsive. The function $\beta\varphi_s$ is a steeply varying function in the vicinity of the particle surface, and therefore so is the total free energy βw. To eliminate discretisation errors in the subsequent analysis, it is important to have $\beta\Delta w(z)$ available on a fine grid in z. This was achieved by fitting, and in all cases a simple function of the form

$$\beta\Delta w(z) = \frac{f_0\left[1-\left(z/z_c\right)^2\right] + f_1 z\left[1-\left(z/z_c\right)\right]}{1+g_1 z+g_2 z^2} \qquad (17)$$

was found to be suitable. This is a ratio of two quadratic functions (a Padé approximant) with the function in the numerator being equal to zero at some cut-off distance z_c. The fit is shown in Figure 3(a), as is the total free energy βw derived from it. The head–surface interaction is, of course, attractive, but the tail–tail interactions are repulsive and the resulting excluded-volume interactions give rise to a significant free-energy barrier to adsorption of approximately 4 k_BT at $z \simeq 2.5\sigma$. Figure 3(b) shows the total free energy curves for $R = 2\sigma$ and $\Gamma\sigma^2 = 0.119$, 0.318, and 0.517. As the surface coverage increases, the depth of the attractive well decreases and the height of the repulsive barrier increases, as a result of increased excluded-volume interactions.

(turn to next page →)

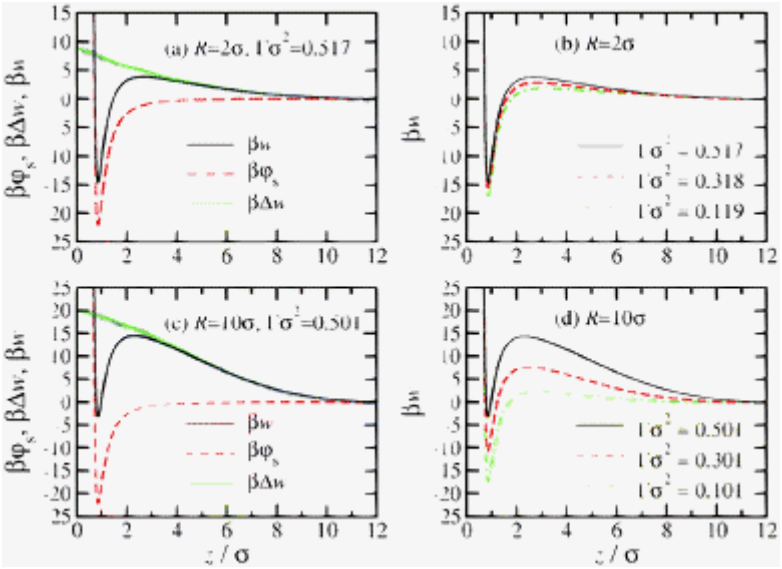

Figure 3. Components of the free energy of adsorption of single surfactant molecules on to surfaces with radius R and coverage $\Gamma\sigma^2$: (a) βw, $\beta\varphi_s$, and $\beta\Delta w$ for $R = 2\sigma$ and $\Gamma\sigma^2 = 0.517$; (b) βw for $R = 2\sigma$ and $\Gamma\sigma^2 = 0.119$, 0.318, and 0.517; (c) βw, $\beta\varphi_s(z)$, and $\beta\Delta w$ for $R = 10\sigma$ and $\Gamma\sigma^2 = 0.501$; (d) βw for $R = 10\sigma$ and $\Gamma\sigma^2 = 0.101$, 0.301, and 0.501. In (a) and (c), the blue crosses are Δw as measured in simulations. The remaining curves are derived from a fit to $\beta\Delta w$ using eqn (17).

Figure 3(c) and (d) show the same data but for a surface with radius $R = 10\sigma$. Firstly, Figure 3(c) shows that the repulsive contribution $\beta\Delta w$ for $\Gamma\sigma^2 = 0.501$ is far greater than that for $R = 2\sigma$ and a similar surface coverage. As a result, the total free energy βw exhibits a far bigger repulsive barrier of height 14 k_BT, and a much smaller attractive region where $w < 0$. The variation of βw with surface coverage is shown in Figure 3(d); again, with increasing surface coverage, the free energy becomes less attractive and the barrier becomes more repulsive, due to the excluded-volume interactions.

There are two contributions to the variation of $\beta\Delta w$ with surface curvature at fixed surface coverage. The first one is due to the effective surface concentration of an adsorbed monolayer, taking in to account the bonding distance of the head group from the surface, as expressed in eqn. (13). For a given surface coverage $\Gamma = N/(4\pi R^2)$, the effective concentration $\Gamma_{\text{eff}} < \Gamma$, with the difference decreasing with increasing radius. Hence, the excluded-volume interactions should be less pronounced for smaller particle radii. This does not account fully for the variations in free energy, as will be shown when the adsorption isotherms are considered in Section 4.2. So, in the mean time, the surface coverage will be characterised by Γ. The second contribution can be understood using the cartoons shown in Figure 2(b) and (c). The diagrams show curved and planar surfaces with strongly adsorbed surfactant molecules *at the same surface coverage*. In the case of the curved surface, the solvophilic tail groups have more available volume due to the diverging radial lines dividing each

molecule from its neighbours. For a colloid of radius R with a surfactant layer of thickness l and surface coverage Γ, the volume per surfactant is

$$v = \frac{1}{4\pi R^2 \Gamma}\left[\frac{4\pi(R+l)^3}{3} - \frac{4\pi R^3}{3}\right] = \frac{l}{\Gamma}\left[1 + \left(\frac{l}{R}\right) + \frac{1}{3}\left(\frac{l}{R}\right)^3\right] \tag{18}$$

which is a monotonically decreasing function of both R and Γ. A free-volume theory could be constructed in which the contribution Δw is represented by a term proportional to $-Nk_BT\ln(v - v_0)$ where v_0 is a close-packed volume-per-molecule. This approach is not taken here, and the focus remains on the accurate numerical results from computer simulations.

Although adsorption kinetics are not the focus of this study, the significant free-energy barriers to adsorption and their dependence on surface curvature and surface coverage should have some interesting consequences for the approach to equilibrium. Starting from empty surfaces, the rate of approach to high equilibrium surface coverages should be slower for flat surfaces than for highly curved surfaces. The physical picture is of a molecule having to penetrate a thick canopy of adsorbed molecules in order for its head group to interact with the surface. Highly curved surfaces should have more exposed volume due to the radial arrangement of the tails, as indicated in Figure 2(b) and (c).

4.2. Adsorption

The adsorption isotherm in eqn. (11) is characterised by the integral

$$K(\Gamma) = \int_0^{z^*}\left(1 + \frac{z}{R}\right)^2 \exp[-\beta w(z)]\mathrm{d}z \tag{19}$$

and so the question is how to choose the cut-off distance z^* which basically delimits the boundary between ‘adsorbed’ and ‘desorbed’ states. Figure 3shows that the total free energy βw possesses a significant global minimum and a local maximum of order 1–10 k_BT in the region of $z = 2$–3σ, depending on curvature and surface coverage. Hence, the running integral with increasing z^* should converge in the region of $z = 2$–3σ. This is demonstrated explicitly in Figure 4, where the logarithm of $K(\Gamma)$ is shown as a function of cut-off distance z. The specific examples given are for $R = 10\sigma$and $\Gamma\sigma^2 = 0.101$, 0.301, and 0.501, *i.e.*, the same data as in Figure 3(d). In all cases, the integrals plateau well before $z^* = 2\sigma$, and so in practice $K(\Gamma)$ can be evaluated with this choice of cut-off distance.

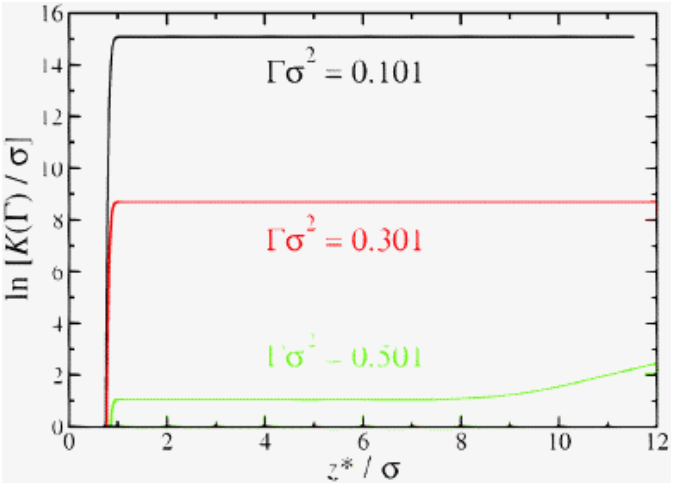

Figure 4. The logarithm of the integral $K(\Gamma)$ from eqn (19) as a function of the cut-off distance z^* separating bound and unbound states. The examples shown are for $R = 10\sigma$ and $\Gamma\sigma^2 = 0.101$, 0.301, and 0.501.

Figure 5 shows the logarithm of the integral $K(\Gamma)$ in eqn (19) calculated as a function of the surface coverage $\Gamma\sigma^2$ for colloid radii $R/\sigma = 2$, 4, 6, 8, and 10. Plotted in this form, there is a roughly linear relationship between ln $K(\Gamma)$ and Γ. Fitted parameters from the equation ln $K(\Gamma) = A + B\Gamma\sigma^2$ are given in Table 1. The $\Gamma \to 0$ limits should be roughly the same for all radii, apart from some minor geometrical effects. The average intercept parameter $A \simeq 18$ with a spread of about ±1. Since the integral $K(\Gamma)$ will be dominated by the contribution from the minimum in $\beta w(z)$, this indicates a typical statistical error in $w(z)$ of about ±1 k_BT, which is reasonable. For a given surface coverage, ln K decreases with increasing surface radius. As explained in Section 3.1, the smaller the value of $K(\Gamma)$, the higher the solution concentration has to be to achieve an equilibrium surface coverage Γ. The decrease in K with increasing Γ arises from the effects of molecular crowding on the surface. This effect is more pronounced with larger radii due to the decrease of available volume per surfactant, as indicated in Figure 2(c).

R/σ	A	B	$\Gamma_{\text{eff}}/\Gamma$
2	17.02(20)	−7.73(61)	0.485
4	17.75(27)	−17.86(89)	0.674
6	18.52(10)	−23.84(28)	0.762
8	17.96(21)	−29.29(70)	0.813
10	18.26(34)	−33.5(1.1)	0.846

Table 1. Fitting parameters for the integral $K(\Gamma) = \exp(A + B\Gamma\sigma^2)$, and the ratio of the effective and actual surface concentrations defined in eqn. (13)

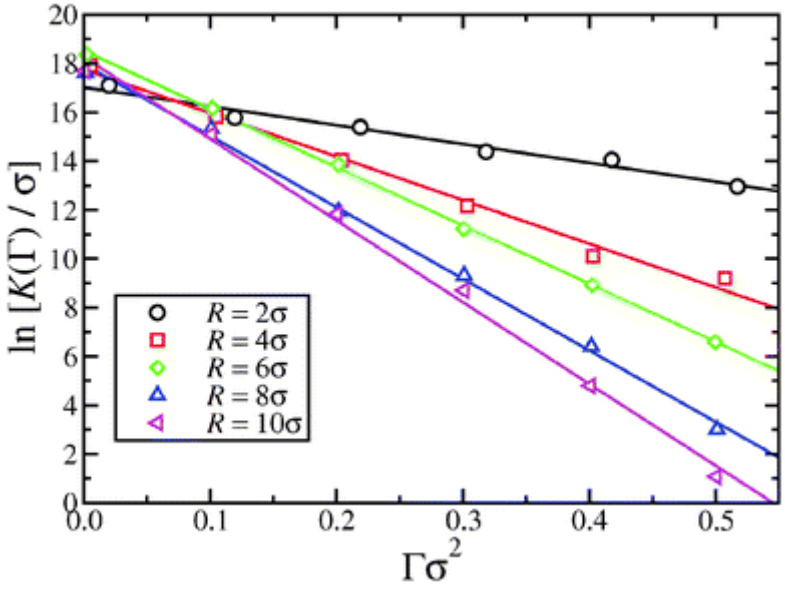

Figure 5. The logarithm of the integral $K(\Gamma)$ from eqn (19) as a function of surface coverage Γ: (black circles) $R = 2\sigma$; (red squares) $R = 4\sigma$; (green diamonds) $R = 6\sigma$; (blue up triangles) $R = 8\sigma$; (magenta left triangles) $R = 10\sigma$. The lines are linear fits, with the parameters given in Table 1.

Figure 6(a) shows the adsorption isotherms [eqn (11)] in the form of $\Gamma\sigma^2$ against $c_0\sigma^3$. For a given solution concentration, the surface coverage increases with decreasing colloid radius. As an example, the surface coverages on surfaces with $R = 2\sigma$ and $R = 10\sigma$ in mutual equilibrium with an ideal solution of concentration $c_0\sigma^3 = 1 \times 10^{-6}$ are $\Gamma\sigma^2 \simeq 0.503$ and 0.183, respectively. To give an idea of real parameters, with $\sigma = 4$ Å, $c_0\sigma^3 = 1 \times 10^{-6}$ corresponds to $c_0 \simeq 26$ μmol L^{-1}. A surface concentration of $\Gamma\sigma^2 = 0.5$ corresponds to an area-per-surfactant of 32 Å. This is an entirely realistic value for detergent-in-oil systems.

(turn to next page →)

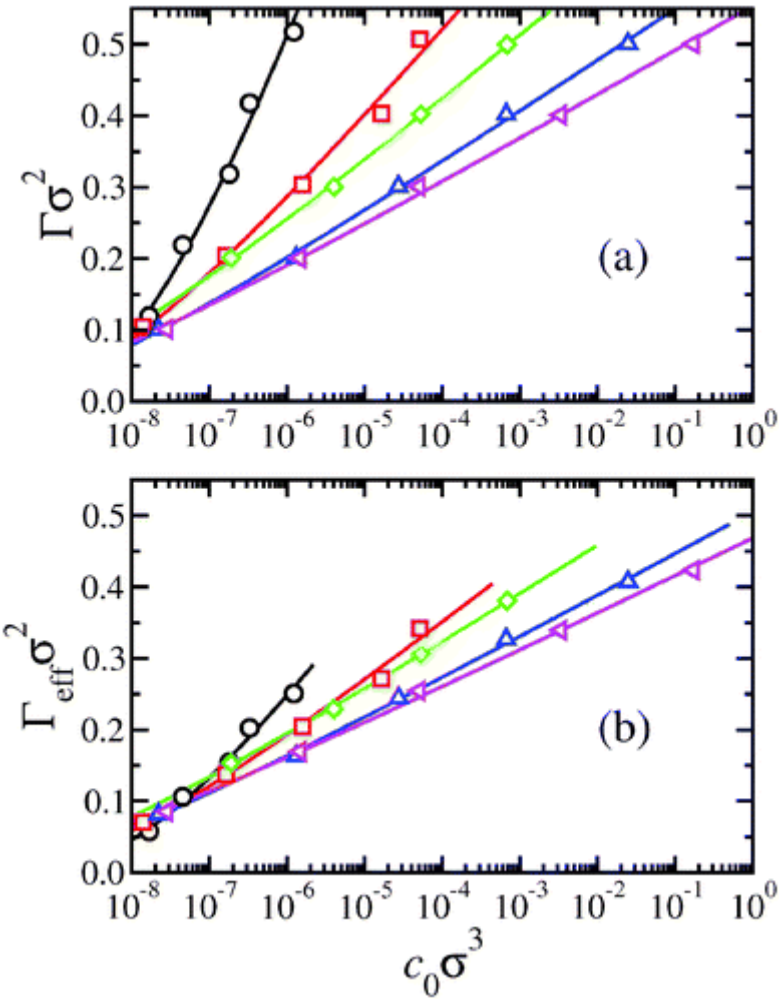

Figure 6. (a) Adsorption isotherms defined by eqn (11) with $K(\Gamma) = \exp(A + B\Gamma\sigma^2)$ and the fit parameters given in Table 1: (black line and circles) $R = 2\sigma$; (red line and squares) colloid with $R = 4\sigma$; (green line and diamonds) colloid with $R = 6\sigma$; (blue line and up triangles) $R = 8\sigma$; (magenta line and left triangles) $R = 10\sigma$. (b) The same isotherms but with the effective surface concentration $\Gamma_{\rm eff}$ given by eqn (13).

Figure 6(a) shows that $\Gamma\sigma^2$ shows a strong dependence on the particle radius, more so than one might anticipate on the basis of the excluded-volume mechanism illustrated in Figure 2(b) and (c). As explained in Section 3.1, the *effective* surface concentration takes account of the distances of the head groups from the surface, and these will be significant for smaller particles. Figure 7 shows the ratio $\Gamma_{\rm eff}/\Gamma$ computed using eqn (13) and the full free-energy profiles βw extracted from simulations. For a given value of R, this ratio shows essentially no variation with surface coverage (actually much less than 1%). The numerical values are given in Table 1. Figure 7 also shows a theoretical curve from the approximation $w(z) = \varphi_s(z)$ (tail contributions are ignored). This is very accurate because the head–surface interaction is so strong compared to the other contributions plotted in Figure 1.

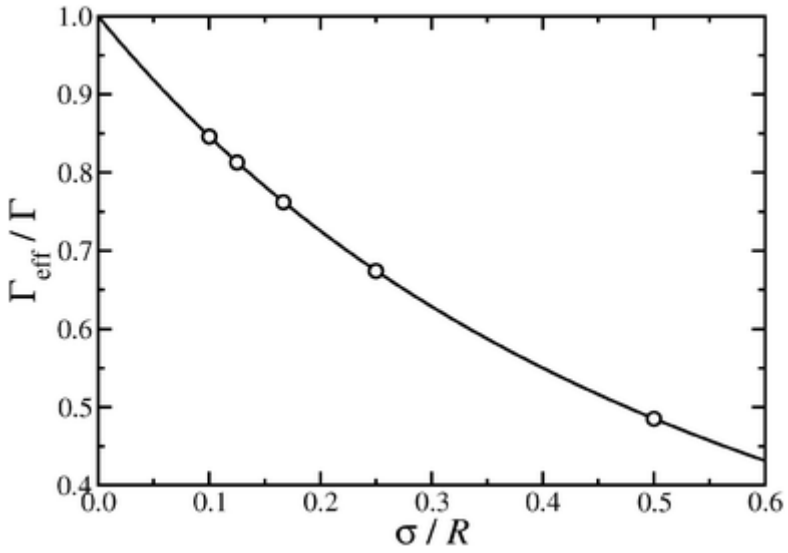

Figure 7. Ratio of the effective surface concentration Γ_{eff} to the nominal value $\Gamma = N/(4\pi R^2)$ as a function of particle radius R, calculated using eqn (13). The points are from simulations and the line is an approximation with $w(z) = \varphi_s(z)$.

Figure 6(b) shows the effective surface concentration as a function of bulk concentration. The variation of Γ_{eff} is less than that of Γ, but there is still a systematic decrease with increasing particle radius. For the same example given above, the effective surface concentrations at $c_0\sigma^3 = 1 \times 10^{-6}$ are $\Gamma_{\mathrm{eff}}\sigma^2 \simeq 0.244$ and 0.155 for $R = 2\sigma$ and $R = 10\sigma$, respectively. This is still a significant effect, no matter how the surface concentration is measured. The variations described here may be significant for practical applications. In a situation where particles are to be introduced in to system to adsorb molecules, then the smaller the particles the better. Not only does this give the best surface area-to-volume ratio, but also the packing of adsorbate on to small particles is greater. In a situation where particles are to be solubilised (such as in overbased detergents), it requires less surfactant per unit area to solubilise a large particle than a small particle. Hence, the total particle mass and total surfactant surfactant could be optimised simultaneously to yield the lowest cost per total particle surface area.

5. Conclusions

The thermodynamics of surfactant adsorption on colloidal surfaces has been studied using coarse-grained models and computer simulations. The models were constructed to isolate the effects of the geometry of the solid–solution interface and the surface coverage. Using an umbrella-sampling technique, the free energy of adsorbing a surfactant molecule from a dilute solution on to a spherical colloid surface has been measured as a function of radius and coverage. The main result is that, for a

given surface coverage, the free energy of adsorption decreases with increasing curvature of the surface. For a given surface curvature, the free energy of adsorption increases with increasing surface coverage. These trends arise from the excluded-volume interactions between the surfactant tails on the surface. The dependence on surface curvature is due to the geometrical increase in available volume for the surfactant tails with decreasing colloid radius. The dependence on surface coverage is due simply to increased tail–tail interactions with increasing coverage. The consequences of these effects on the equilibrium partitioning of surfactant between different types of surface have been outlined. These observations suggest that, all other things being equal, the presence of different curvature surfaces in a heterogeneous system could be enough to stabilise an uneven distribution of adsorbate between surfaces.

Future work will move in three directions. Firstly, the methodology employed here will be applied to atomistic models with explicit solvent, in order to resolve the effects of specific chemical interactions and desolvation on the adsorption free-energy profile. Secondly, coarse-grained models will be extended to take account of differences in surfactant shape. For example, wedge-shaped molecules with small head groups and multiple tails may adsorb preferentially on a surface with a specific curvature that optimises the molecular packing. Finally, competitive adsorption between several different surfactants may be examined by mapping out the free energy of adsorption as a function of the individual surface coverages.

References

[1] P. G. Cummins, E. Staples and J. Penfold, *J. Phys. Chem.*, 1990, **94**, 3740–3745.

[2] P. G. Cummins, J. Penfold and E. Staples, *J. Phys. Chem.*, 1992, **96**, 8092–8094.

[3] J. Penfold, E. Staples, I. Tucker and P. Cummins, *J. Phys. Chem.*, 1996, **100**, 18133–18137.

[4] J. Penfold, E. J. Staples, I. Tucker and L. J. Thompson, *Langmuir*, 1997, **13**, 6638–6643.

[5] J. Penfold, E. J. Staples, I. Tucker and R. K. Thomas, *Langmuir*, 2000, **16**, 8879–8883.

[6] J. Penfold, E. Staples, I. Tucker and R. K. Thomas, *Langmuir*, 2002, **18**, 5755–5760.

[7] P. E. Levitz, *Colloids Surf., A*, 2002, **205**, 31–38.

[8] G. Despert and J. Oberdisse, *Langmuir*, 2003, **19**, 7604–7610.

[9] J. Penfold, I. Tucker and R. K. Thomas, *Langmuir*, 2005, **21**, 6330–6336.

[10] D. Lugo, J. Oberdisse, M. Karg, R. Schweins and G. H. Findenegg, *Soft Matter*, 2009, **5**, 2928–2936.

[11] D. M. Lugo, J. Oberdisse, A. Lapp and G. H. Findenegg, *J. Phys. Chem. B*, 2010, **114**, 4183–4191.

[12] K. P. Sharma, V. K. Aswal and G. Kumaraswamy, *J. Phys. Chem. B*, 2010, **114**, 10986–10994.

[13] B. Bharti, J. Meissner, U. Gasser and G. H. Findenegg, *Soft Matter*, 2012, **8**, 6573–6581.

[14] S. Kumar, V. K. Aswal and J. Kohlbrecher, *Langmuir*, 2012, **28**, 9288–9297.

[15] C. A. Bearchell, T. N. Danks, D. M. Heyes, D. J. Moreton and S. E. Taylor, *Phys. Chem. Chem. Phys.*, 2000, **2**, 5197–5207.

[16] C. A. Bearchell, D. M. Heyes, D. J. Moreton and S. E. Taylor, *Phys. Chem. Chem. Phys.*, 2001, **3**, 4774–4783.

[17] L. K. Shrestha, R. G. Shrestha, M. Abe and K. Ariga, *Soft Matter*, 2011, **7**, 10017–10024.

[18] Z. Xu, X. Yang and Z. Yang, *J. Phys. Chem. B*, 2008, **112**, 13802–13811.

[19] C. P. O'Brien, S. J. Stuart, D. A. Bruce and R. A. Latour, *Langmuir*, 2008, **24**, 14115–14124.

[20] V. Vivcharuk, B. Tomberli, I. S. Tolokh and C. G. Gray, *Phys. Rev. E*, 2008, **77**, 031913.

[21] N. R. Tummala and A. Striolo, *Phys. Rev. E*, 2009, **80**, 021408.

[22] T. Zehl, M. Wahab, P. Schiller and H.-J. Mögel, *Langmuir*, 2009, **25**, 2090–2100.

[23] F. Tian, Y. Luo and X. Zhang, *J. Chem. Phys.*, 2010, **133**, 144701.

[24] D. Chandler, *Introduction to modern statistical mechanics*, Oxford University Press, Oxford, 1987.

[25] J. G. Kirkwood, *J. Chem. Phys.*, 1935, **3**, 300–313.

[26] S. Kawai and T. Komatsuzaki, *Phys. Rev. E*, 2013, **87**, 030803(R).

[27] J. D. Weeks, D. Chandler and H. C. Andersen, *J. Chem. Phys.*, 1971, **54**, 5237–5247.

[28] G. S. Grest and K. Kremer, *Phys. Rev. A*, 1986, **33**, 3628–3631.

[29] G. S. Grest, K. Kremer and T. A. Witten, *Macromolecules*, 1987, **20**, 1376–1383.

[30] G. S. Grest, M.-D. Lacasse, K. Kremer and A. M. Gupta, *J. Chem. Phys.*, 1996, **105**, 10583–10594.

[31] S. W. Sides, G. S. Grest and M. J. Stevens, *Macromolecules*, 2002, **35**, 566–573.

[32] A. Chremos, E. Glynos, V. Koutsos and P. J. Camp, *Soft Matter*, 2009, **5**, 637–645.

[33] D. Ambrose and C. Tsonopoulos, *J. Chem. Eng. Data*, 1995, **40**, 531–546.

[34] W. Shi and J. K. Johnson, *Fluid Phase Equilib.*, 2001, **187–188**, 171–191.

[35] M. P. Allen and D. J. Tildesley, *Computer simulation of liquids*, Clarendon Press, Oxford, 1987.

[36] J. S. Rowlinson and B. Widom, *Molecular Theory of Capillarity*, Dover Publications, Inc., Mineola, New York, 2002.

[37] G. M. Torrie and J. P. Valleau, *J. Comput. Phys.*, 1977, **23**, 187–199.